Ring localized structures in nonlinear shallow water wave dynamics

2014 J. Phys.: Conf. Ser. 482 012030

(http://iopscience.iop.org/1742-6596/482/1/012030)

Physics and Mathematics of Nonlinear Phenomena 2013 (PMNP2013) IOP Publishing
Journal of Physics: Conference Series **482** (2014) 012030 doi:10.1088/1742-6596/482/1/012030

Ring localized structures in nonlinear shallow water wave dynamics

A. Mannan[1,6], R. Fedele[2,6], M. Onorato[3], S. De Nicola[4,6] and D. Jovanović[5,6]

[1] Dipartimento di Matematica e Fisica, Seconda Università degli Studi di Napoli, Sede di Caserta, Caserta, Italy
[2] Dipartimento di Fisica, Università di Napoli "Federico II", Napoli, Italy
[3] Dipartimento di Fisica, Università di Torino, Torino, Italy
[4] CNR-SPIN Napoli, Napoli, Italy
[5] Institute of Physics, University of Belgrade, Belgrade, Serbia
[6] INFN Sezione di Napoli, Napoli, Italy

E-mail: abdul.mannan@na.infn.it

Abstract. The nonlinear dynamics of the concentric shallow water waves is described by means of the *cylindrical* Korteweg-de Vries equation, often referred to as the *concentric* Korteweg-de Vries equation (cKdVE). By using the mapping that transforms a cKdVE into the standard one – hereafter also referred to as the *planar* Korteweg-de Vries equation (KdVE) – the spatiotemporal evolution of a cylindrical surface water wave, corresponding to a *tilted* cylindrical bright soliton, is described. The usual representation of a tilted soliton is 'non-physical'; here the cylindrical coordinate and the retarded time play the role of time-like and space-like variables, respectively. However, we show that, when we express such analytical solution of the cKdVE in the appropriate representation in terms of the two horizontal space coordinates, say X and Y, and the 'true' time, say T, this non-physical character disappears. The analysis is then carried out numerically to consider the surface water wave evolution corresponding to initially localized structures with standard boundary conditions, such as bright soliton, Gaussian and Lorentzian profiles. A comparison among those profiles is finally presented.

1. Introduction

Large amplitude wave propagation is encountered in almost all physical areas, ranging from nano- to astro-physical scales [1, 2, 3, 4, 5]. Remarkably, in such diverse areas, most of the nonlinear physical processes involved in the nonlinear wave propagation are modeled by similar nonlinear partial differential equations. The physics of extreme events, or simply the *extreme physics*, is a very recently-developed interdisciplinary research area, based on a very wide platform of phenomena and methodologies that are imported from the diverse disciplines. For instance, ultra-strong wave intensities can be artificially produced by means of very advanced techniques, such as the use of ultra-short (duration in femto-seconds and, in the near future, atto-seconds and ultra strong ($10^{20} - 10^{22}$ W/cm^2 intensities) laser pulses [6, 7] in plasmas to achieve the particle acceleration to very high energies (plasma-based accelerator schemes) [6, 7, 8, 9] or the controlled thermonuclear inertial fusion [10]. Ultra-strong wave intensities can be also naturally generated, such as in a number of astrophysical conditions [11, 12] or in ocean wave physics [13]. The latter is essentially the physics of the surface gravity waves, ranging

from shallow to deep water regimes, and it is probably the oldest discipline deeply related to the extreme physics [14], such as the one involving rogue wave [15] and tsunami generation [16]. However, water wave physics, that includes also the study of artificially-produced nonlinear wave phenomena, is the subject for which several mathematical techniques to analyze and solving nonlinear partial differential equations have been developed for the first time and, later on, transferred to the other disciplines.

In this paper, we describe the dynamics of concentric large amplitude surface gravity waves in shallow water regime, in the horizontal space coordinates. This is done both analytically and numerically. In particular, the analytical description is done by using the mapping that relates the analytical solutions of the concentric (or cylindrical) Korteweg-de Vries equation (cKdVE) to the ones of the standard (or planar) Korteweg-de Vries equation (KdVE). Then, we analyze numerically the spatiotemporal evolution of cylindrical localized surface gravity waves with different initial profiles (f. i., bright soliton, Gaussian and Lorentzian). In the next section, we briefly review the fluid model typically adopted to obtain both the families of the KdVE and cKdVE describing the nonlinear water waves in the shallow water regime. In section 3, we briefly present the transformation that allows to go from cKdVE to KdVE and vice versa. Then the analytical nonlinear shallow water solutions of cKdVE with *tilted* boundary conditions are found: they are the image of the localized shallow water solutions of the planar KdVE by means of the above mapping. In section 4, we find concentric numerical solutions of the cKdVE, corresponding to bright, Gaussian and Lorentzian initial profiles. All the solutions are first represented in the retarded time and the radial space coordinates (ζ and s, respectively). Once these variables are expressed in the horizontal ones, X and Y, all the above solutions assume the form of ring localized structures (vortex state) characterized by a cylindrical propagation which is associated with a decreasing of the amplitude as $1/s$. Finally, conclusions and remarks are given in section 5.

2. Model equations

We assume the model of water corresponding to an incompressible, inviscid fluid of constant density ρ with the acceleration of gravity g and a zero surface tension. We also assume that the water moves over an impermeable bed with constant depth and with a constant pressure (atmospheric pressure) at the free surface. To write the governing equations of our system, we refer for procedure and details to the previous literature [f. i., see [17, 18, 19], and references therein]. These consist in the Euler's equations of motion (separated into vertical and perpendicular components with respect to the direction of the gravity acceleration vector $\mathbf{g}$) and mass conservation equation. These can be cast as follows

$$\frac{\partial \mathbf{v}_\perp}{\partial t} + \epsilon(\mathbf{V}\cdot\nabla)\mathbf{v}_\perp = -\nabla_\perp p, \tag{1}$$

$$\delta^2\left[\frac{\partial w}{\partial t} + \epsilon(\mathbf{V}\cdot\nabla)w\right] = -\frac{\partial p}{\partial z}, \tag{2}$$

$$\nabla\cdot\mathbf{V} = 0, \tag{3}$$

where: z is the vertical component of the position vector normalized to the constant unperturbed depth h_0; $\nabla = \nabla_\perp + \hat{z}\partial/\partial z$ is the gradient operator, $\nabla_\perp$ being its perpendicular component; p denotes the dimensionless pressure which measures the deviation from the hydrostatic pressure distribution; $\mathbf{V} = (\mathbf{v}_\perp, w)$ is the fluid velocity, $\mathbf{v}_\perp$ and w being the perpendicular component normalized by $\sqrt{gh_0}$ and the vertical component normalized by $h_0\sqrt{gh_0}/\lambda$, respectively, with λ wavelength of the wave; t is the time variable normalized by $\lambda/\sqrt{gh_0}$. Note that, by denoting by $\mathbf{x}_\perp$ as the perpendicular component of the position vector normalized by λ, $z = h(\mathbf{x}_\perp, t)/h_0$ represents the surface normalized by h_0, h being the actual depth. Equations (1)-(3) have been

written by introducing some parameters that fix the scales of the problem. First of all, we have defined the parameter $\delta = h_0/\lambda$ which estimates the shallowness of the water and introduced an arbitrarily large perturbation in height, namely $h(\mathbf{x}_\perp, t) = h_0 + \Delta h(\mathbf{x}_\perp, t)$. Then, denoting by a the maximum value of Δh, we have defined the dimensionless quantity $\eta(\mathbf{x}_\perp, t) = \Delta h(\mathbf{x}_\perp, t)/a$, which represents the profile of the perturbation, usually referred to as the *elevation* of the surface wave. Therefore, the expression for h can be easily rewritten, i.e., $h(\mathbf{x}_\perp, t) = h_0 + a\eta(\mathbf{x}_\perp, t)$ and another fundamental parameter has been introduced, i.e., $\epsilon = a/h_0$, that gives the measure of the nonlinearity (i.e. estimates how large is the amplitude).

Note that, if $\epsilon = 0$ no wave is present. Consequently, as $\epsilon \to 0$, the disturbances associated with the passage of the wave vanish. However, when ϵ increases the amplitude of the perturbations becomes larger, so that $\epsilon \ll 1$ describes the linear regime, whilst the values closer to 1 describe the nonlinear regime. It turns out, that, in order to be consistent with the choice of the ϵ value, it is required that we scale our physical quantity with respect to ϵ as follows: $(\mathbf{v}_\perp, w, p) \to \epsilon(\mathbf{v}_\perp, w, p)$. Equations (1)-(3) have to be implemented by the following boundary conditions with

$$p = \eta \quad and \quad w = \frac{\partial \eta}{\partial t} + \epsilon(\mathbf{v}_\perp \cdot \nabla_\perp)\eta \quad on \quad z = 1 + \epsilon\eta \tag{4}$$

and

$$w = 0 \quad on \quad z = 0. \tag{5}$$

Boundary condition (4) corresponds to impose that the pressure on the wave surface be the atmospheric pressure and the vertical velocity component is given by the total derivative of the elevation, whilst the boundary condition (5) fixes to 0 the vertical velocity component at the bottom.

2.1. Korteweg-de Vries equation

To derive the KdVE, we assume that a fluid disturbance is propagating in a narrow channel with $\mathbf{x}_\perp = (x, y)$ and $\mathbf{v}_\perp = (u_x, 0)$ (absence of $y-$component of the transverse velocity field $\mathbf{v}_\perp$), and that all quantities depends only on x, z and t. Moreover, the effects of surface tension are assumed to be negligible. We further introduce the new variables $\mathbf{X}_\perp$, T and W, by the following scaling

$$\mathbf{x}_\perp = \frac{\delta}{\sqrt{\epsilon}}\mathbf{X}_\perp \equiv \frac{\delta}{\sqrt{\epsilon}}(X, Y), \quad t = \frac{\delta}{\sqrt{\epsilon}}T, \quad w = \frac{\sqrt{\epsilon}}{\delta}W\,. \tag{6}$$

By substituting this scaling in eqs. (1)-(5), we obtain the governing system of equations which is similar to the former one, but where δ^2 is replaced by ϵ. For disturbances that are propagating in the positive X-direction, we introduce the following stretched coordinates:

$$\xi = X - \tau, \quad \tau = \epsilon\, T\,. \tag{7}$$

Note that τ describes the long time scale. We restrict our study to a weakly nonlinear evolution equation and perform a Taylor expansion in the small parameter ϵ of η, u_x, W, and p. After some tedious calculations (for details, see Ref. [17]), we finally obtain an equation for η_0 (the surface elevation at the leading order):

$$\frac{\partial \eta_0}{\partial \tau} + \frac{3}{2}\eta_0 \frac{\partial \eta_0}{\partial \xi} + \frac{1}{6}\frac{\partial^3 \eta_0}{\partial \xi^3} = 0. \tag{8}$$

Equation (8), usually referred to as the Korteweg-de Vries equation, governs the spatio-temporal evolution of surface waves in shallow water.

2.2. Cylindrical Korteweg-de Vries equation

In cylindrical coordinates (r, θ, z), with the z-axis pointing upwards in the vertical direction, the flow region is bounded below by solid bottom at $z = 0$, and above by a free surface, say $z = \eta(r, t)$, which measures the displacement from the undisturbed free surface at $z = 0$. The fluid is supposed to be unbounded in the radial direction ($0 < r < \infty$). Here, the cylindrical coordinates are dimensionless as in the previous case. The perpendicular components $\mathbf{x}_\perp$ of the position vector $\mathbf{x}$ is here represented by $\mathbf{x}_\perp = (r, \theta)$. For simplicity, we consider long waves having a vertical axis of symmetry at all values of the time t (cylindrical symmetry). So that, the governing equations describe surface waves with a circular wave front. Therefore, all the quantities are independent of θ and the perpendicular component of the velocity field is only radial, say u_r. To determine the cylindrical KdVE, we follow a procedure similar to the one used for the KdVE case. Thus, we introduce the stretched coordinates, ζ (retarded time) and s, and new variables H, P, U, W, respectively, i.e.

$$\zeta = \frac{\epsilon^2}{\delta^2}(r - t), \quad s = \frac{\epsilon^6}{\delta^4} r, \quad (\eta, p, u_r) = \frac{\epsilon^3}{\delta^2}(H, P, U), \quad w = \frac{\epsilon^5}{\delta^4} W. \tag{9}$$

in the governing eqs. (1)-(5). Following the weakly nonlinear analysis performed in the one dimensional case (for details see Ref. [17]), we get for the leading order term, say H_0, the following equation:

$$\frac{\partial H_0}{\partial s} + \frac{3}{2} H_0 \frac{\partial H_0}{\partial \zeta} + \frac{1}{6} \frac{\partial^3 H_0}{\partial \zeta^3} + \frac{H_0}{2s} = 0. \tag{10}$$

Equation (10) is usually referred to as the concentric Korteweg-de Vries equation.

3. Analytical soliton solutions for cylindrical surface gravity waves

In order to describe analytically the spatiotemporal evolution of the surface gravity waves in the form of solitons, we use the connection between eqs. (8) and (10). Let us take their more general forms, where the coefficients $3/2$ and $1/6$ are replaced by arbitrary coefficients A and B, respectively, that are assumed to be real numbers. For simplicity of the notation, we introduce also the following replacements: $\eta_0 \to u$ and $H_0 \to v$. Then, we consider the following planar and cylindrical Korteweg-de Vries equations, respectively:

$$\frac{\partial u}{\partial \tau} + B\, u \frac{\partial u}{\partial \xi} + A \frac{\partial^3 u}{\partial \xi^3} = 0 \tag{11}$$

and

$$\frac{\partial v}{\partial s} + B\, v \frac{\partial v}{\partial \zeta} + A \frac{\partial^3 v}{\partial \zeta^3} + \frac{v}{2s} = 0\,. \tag{12}$$

According to the definitions given in the previous sections, all the quantities involved in these equations are dimensionless. It is easy to see that eqs. (11) and (12) are related by the following transformations [20, 21]:

$$\mathcal{T} : \begin{cases} \xi = s^{-1/2}\zeta, \quad \tau = -2s^{-1/2} \\ v(\zeta, s) = s^{-1}\left[u\left(\xi = s^{-1/2}\zeta, \tau = -2s^{-1/2}\right) + \zeta/2B\right] \end{cases} \tag{13}$$

and

$$\mathcal{T}' : \begin{cases} \zeta = -2\xi/\tau, \quad s = 4/\tau^2 \\ u(\xi, \tau) = \tau^{-1}\left[4\tau^{-1} v\left(\zeta = -2\xi/\tau,\, s = 4/\tau^2\right) + \xi/B\right] \end{cases}. \tag{14}$$

Note that $\mathcal{T}$ transforms (11) into (12) whilst $\mathcal{T}'$ transforms (12) into (11). A transformation similar to $\mathcal{T}'$ have been first introduced in Ref. [22].

Remarkably, similar transformations have been found to transform the planar to the cylindrical Kadomtsev-Petviashvili equations [23].
To find an analytical solutions of the cKdVE, we consider here the classical planar bright soliton:

$$u(\xi,\tau) = u_m \,\mathrm{sech}^2\left[\sqrt{\frac{B u_m}{12A}}\,(\xi - V_0\tau)\right], \tag{15}$$

where $B\,u_m/A > 0$, and $V_0 = B\,u_m/3$.
By using the transformation (13), we find the solutions of the concentric equation (12) corresponding to the bright soliton of the planar KdVE. By definition, we may refer these concentric solutions to as the *cylindrical (or concentric) bright soliton*, with tilted boundary conditions. Therefore, we have:

$$v(\zeta,s) = \frac{1}{B\,s}\left\{\frac{1}{2}\zeta + B\,u_m\,\mathrm{sech}^2\left[\sqrt{\frac{B\,u_m}{12A\,s}}\,(\zeta + 2V_0)\right]\right\}, \tag{16}$$

where, according to (13) and (14), the standard boundary conditions of solitons (15) are transformed into *tilted* boundary conditions by means of transformation $\mathcal{T}$. The analytical

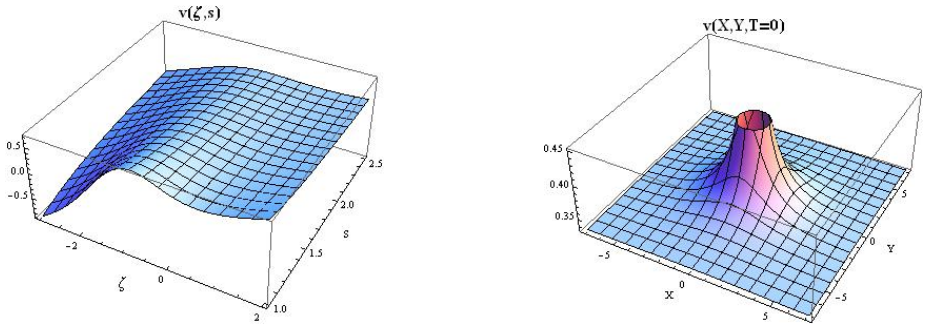

Figure 1. 3D spatial profile of the height v of the analytical initial bright soliton in true space (ζ,s) and X-Y plane for $u_m = 1.0$, $A = 1/6$, and $B = 3/2$.

concentric single-soliton solutions are displayed in figures 1 and 2. The plot on the left side of figure 1 represents tilted solitons as a function of ζ and s. The 3D plot on the right side of figure 1 shows the corresponding solutions in the $X - Y$ space at $T = 0$ (note that the cylindrical coordinate $s \propto \sqrt{X^2 + Y^2}$ corresponds to the time-like variable for cKdVE). Figure 2 shows the temporal evolution (in $T \propto t$) of the 3D plots in the $X - Y$ plane for a tilted-bright soliton. We observe that the initial profiles ($T = 0$) *radiate* circularly. This is due to the non-stationary features of the tilted-solitons with respect to the artificial time s.

4. Numerical solutions of the cylindrical case

We consider three different initial conditions: the bright soliton case given by eq. (17), the Gaussian and the Lorentzian profiles given by eqs. (18) and (19), respectively. The parameter s_i in each case governs the width of the three distributions at the initial time.

$$v(\zeta) = \frac{u_m}{s_i}\mathrm{sech}^2\left[\zeta\sqrt{\frac{B u_m}{12A s_i}}\right], \tag{17}$$

$$v(\zeta) = \frac{u_m}{s_i}\exp\left[-\left(\frac{\zeta}{s_i}\right)^2\right], \tag{18}$$

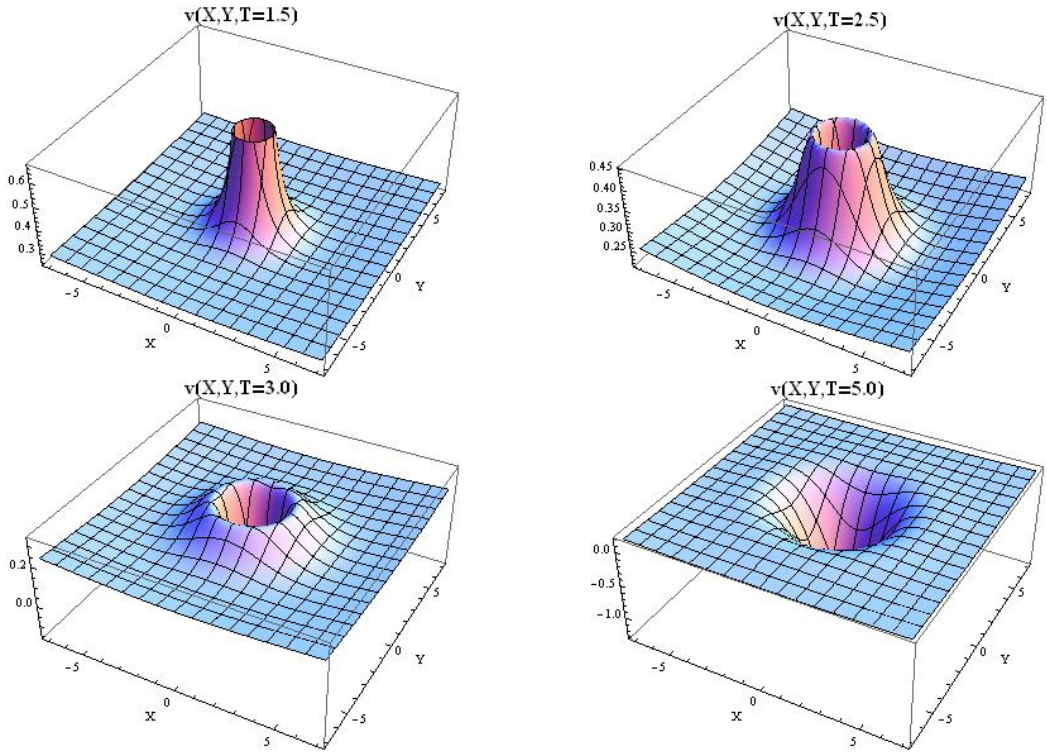

Figure 2. 3D spatial profile of the height v of the analytical bright soliton in X-Y plane for $u_m = 1.0$, $A = 1/6$, and $B = 3/2$.

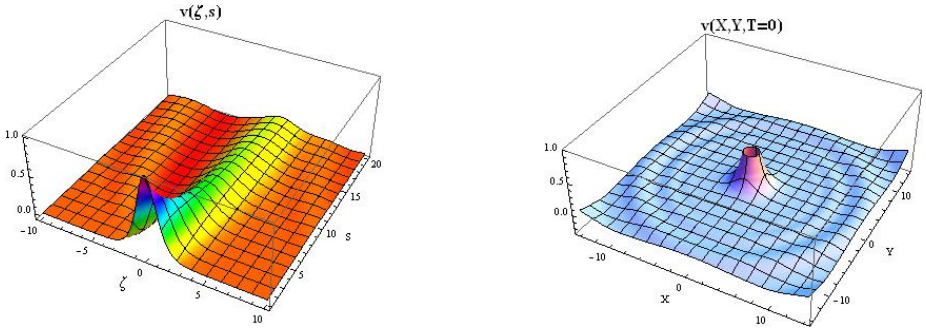

Figure 3. 3D spatial profile of the height v of the initial bright soliton in true space (ζ,s) and X-Y space for $u_m = 1.0$, $A = 1/6$, and $B = 3/2$.

$$v(\zeta) \quad = \quad \frac{u_m/s_i}{1 + (\zeta/s_i)^2}. \tag{19}$$

The plot on the left side of figure 3 displays the numerical calculation of the 3D spatial profile of the height of the cylindrical bright soliton in true space. The numerical results have been obtained by integrating the eq. (12) with standard boundary conditions. The corresponding representation of the 3D profile of the height is represented in the real $X - Y$ plane at the true time $T = 0$ and it is shown on the right side of figure 3 for the same values of the parameters $u_m = 1.0$, $A = 1/6$, and $B = 3/2$. Figure 4 shows the time evolution of the 3D spatial profile of the height of the cylindrical bright soliton in $X - Y$ plane for increasing the values of the true time T. The amplitude of the localized initial profile decreases with increasing the time

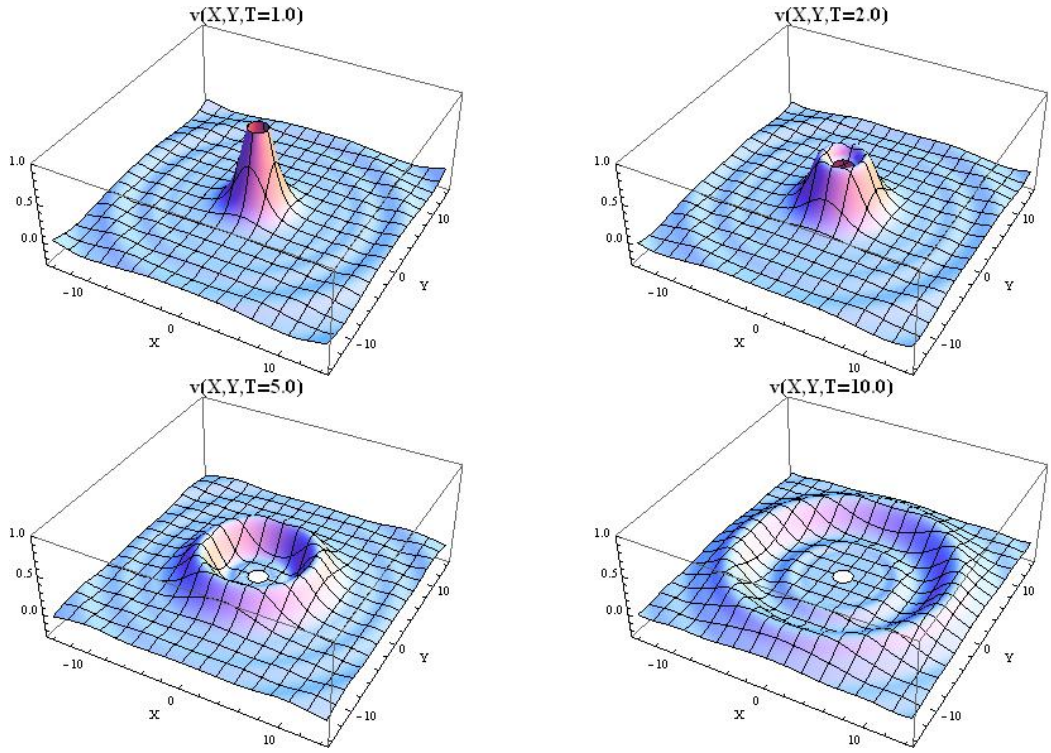

Figure 4. 3D spatial profile of the height v of the bright soliton in X-Y space for $u_m = 1.0$, $A = 1/6$, and $B = 3/2$.

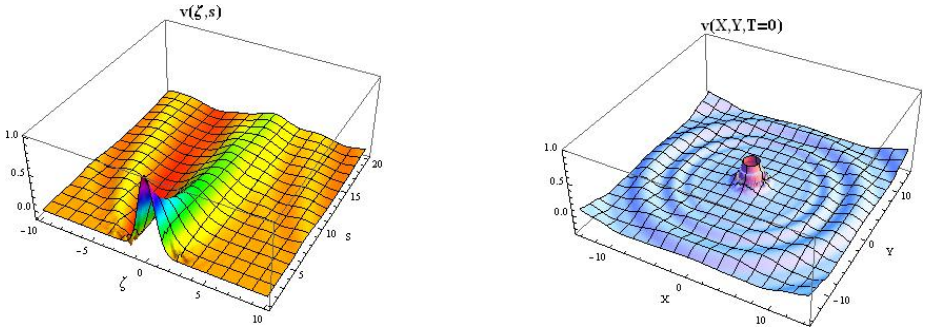

Figure 5. 3D spatial profile of the height v of the initial Gaussian case in true space (ζ,s) and X-Y space for $u_m = 1.0$, $A = 1/6$, and $B = 3/2$.

T while the waves are radiated in a form of circular front in the $X - Y$ plane. Figures 5, 6, 7, and 8 show the results of the numerical integration of eq. (12) for Gaussian and Lorentzian initial conditions given by the eqs. (18) and (19), respectively. It can be clearly seen that the initial peaked amplitude decreases rapidly with increasing time T. Both the initial profiles tend to radiate in circular front with increasing radii. However the radiation emitted in the case of the initial Lorentzian profile appeared to be less pronounced compared to the Gaussian case and resulting in the formation of circular front comparable to the bright soliton case.

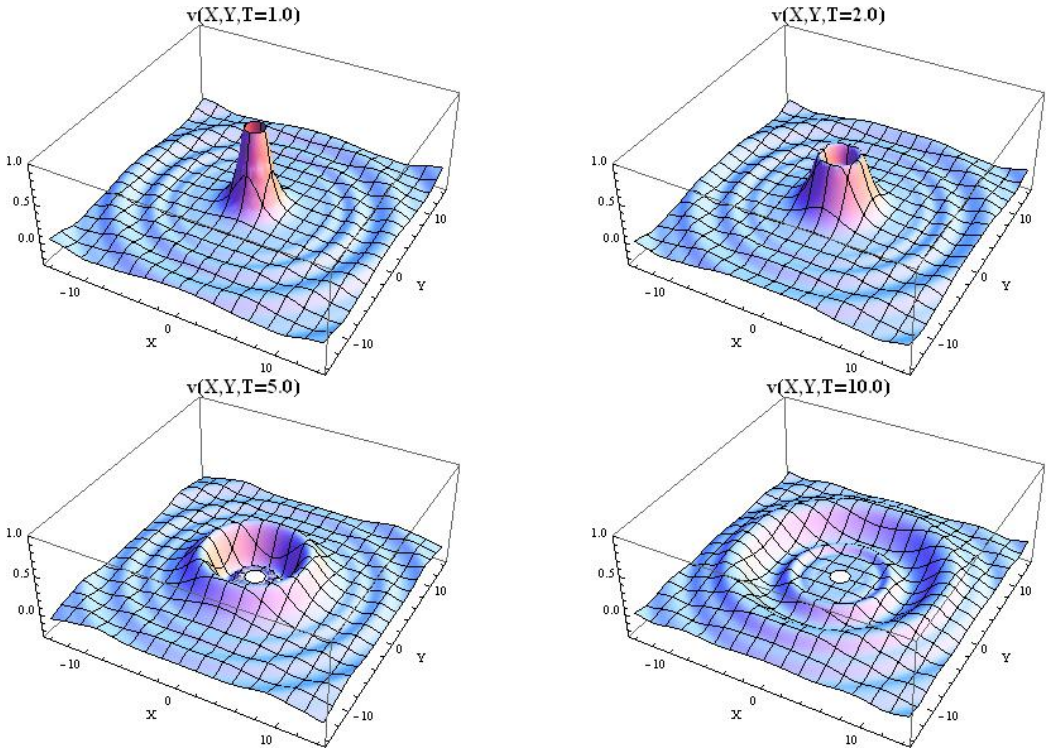

Figure 6. 3D spatial profile of the height v of the Gaussian profile in X-Y space for $u_m = 1.0$, $A = 1/6$, and $B = 3/2$.

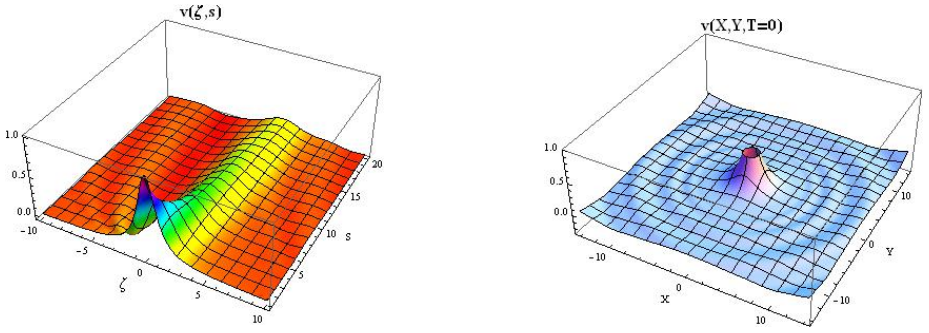

Figure 7. 3D spatial profile of the height v of the initial Lorentzian case in true space (ζ,s) and X-Y plane for $u_m = 1.0$, $A = 1/6$, and $B = 3/2$.

5. Conclusions and remarks

In this paper, we have studied both analytically and numerically, the nonlinear dynamics of the concentric surface gravity waves in the form of localized solutions of the cylindrical KdVE. We have also reviewed the previous approaches, by using a transformation that relates the solutions of the planar (or standard) KdVE to those of the cKdVE. The analytical localized solution (in the $\zeta - s$ domain) in the form of bright tilted solitons has been found. These solutions have also been represented in the real $X - Y$ space and in the true time T, where the spatio-temporal evolution of the tilted solitons ($\zeta - s$ representation) is transformed to X-Y space with an initially given ($T = 0$) soliton profile. The "temporal" behavior with respect to the time-like variable s shows that the localized shape of the analytical solutions reduces as s increases, vanishing

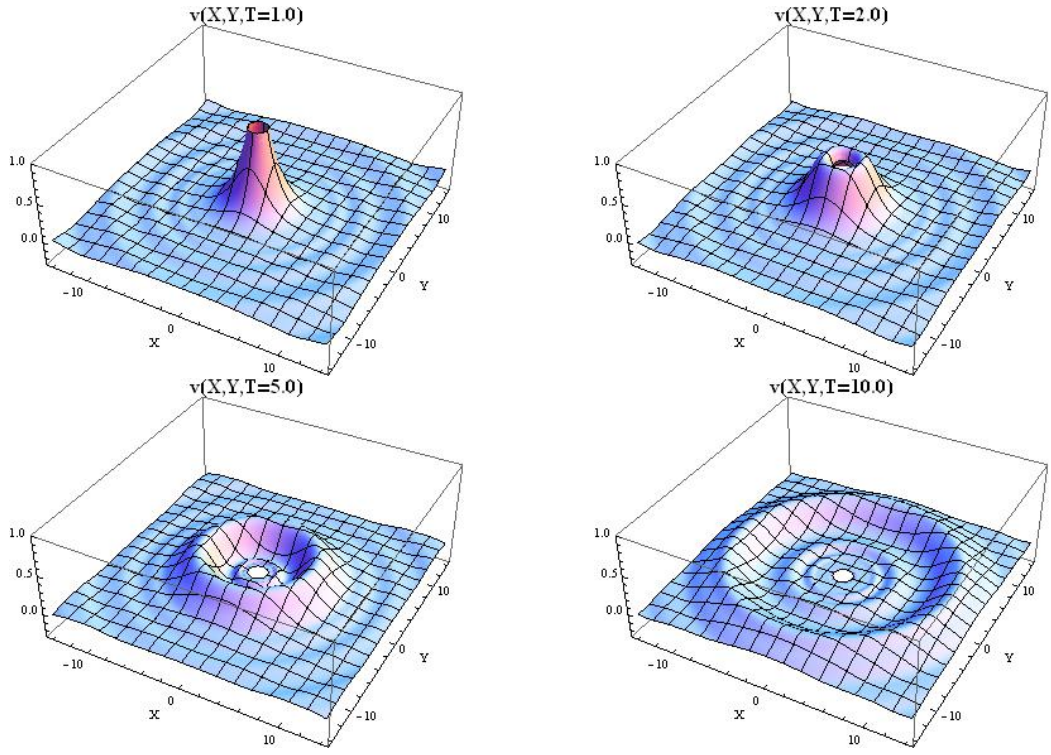

Figure 8. 3D spatial profile of the height v of the Lorentzian profile in X-Y plane for $u_m = 1.0$, $A = 1/6$, and $B = 3/2$.

asymptotically; correspondingly, the tilted character of these solutions reduces as s increases, as well, for asymptotic values of s. Numerical localized solutions with standard boundary conditions corresponding to single-pulse initial profiles, has been found as function of ζ and s. They show a temporal behavior (with respect to s) of the local amplitude similar to the one shown by the analytical localized solutions. Also here this behavior is transformed to $X - Y$ space with an initially given localized profile ($T = 0$). Furthermore, we observe that the analytical solutions of the cKdVE (with *tilted* character) and the numerical ones (with *standard* character of the boundary conditions), both given in $\zeta - s$ space, when transformed to the $(X - Y)$ space, show very similar behavior during the propagation. In particular they exhibit similar features of ring localized structures (in particular, ring bright solitons) that are typically associated with vortex states. Remarkably, this physical circumstance was observed in an irrotational medium.

Finally, we would like to stress that, in this preliminary investigation, we have analysed only the behaviour of localized structures that assume the form of a single pulse in the $\zeta - s$ domain. However, a more detailed analysis, that takes into account both analytical and numerical localized structures, in the form of multi-pulses (in particular, multi-solitons), in $\zeta - s$ domain, is under way. In this space, the simple typical feature exhibited by the *planar* multi-pulse structures, for which the higher pulses have the higher speed, becomes more complex or not easily recognizable for concentric waves, and in the tilted analytical solutions is *apparently* lost. Furthermore, once such structures are transformed to the $X - Y$ space, this nonlinear feature seems to be hidden by the ring character of the waves in this representation. In a forthcoming paper, we analyse in detail all these aspects.

References

[1] Witham G B 1974 *Linear and nonlinear waves* (John Wiley, New York)

[2] Calogero F and Degasperis A 1982 *Spectral transform and solitons* (North-Holland, Amsterdam) vol. I
[3] Dodd R K, Eilbeck J C, Gibbon J D and Morris H C 1982 *Soliton and nonlinear wave equations* (Academic Press, London)
[4] Karpman V I 1975 *Nonlinear Waves in Dispersive Media* (Pergamon Press, Oxford)
[5] Sulem C and Sulem P L 1999 *The Nonlinear Schrödinger Equation: Self-focusing and Wave Collapse* (Springer, New York)
[6] Koke S *et al.* 2010 *Nature Photonics* **4** 462
[7] Jovanović D, Fedele R, Tanjia F, De Nicola S and Gizzi L A 2012 *Eur. Phys. J. D* **66** 328
[8] Esarey E, Sprangle P, Krall J and Ting A 1996 *IEEE Trans. Plasma Sci.* **24** 253, and references therein
[9] Bingham R, Mendosça J T and Shukla P K 2004 *Plasma Phys. Control. Fusion* **46** R1, and references therein
[10] Atzeni S and Meyer-ter-Vehn J 2004 *The Physics of Inertial Fusion* (Oxford University Press, New York)
[11] http://www.astro.cornell.edu/extreme-physics-and-astrophysics-of-compact-objects.html
[12] http://www.eli-beams.eu/eli-events/relativistic-laboratory-astrophysics-with-extreme-power-lasers/
[13] Kharif C, Pelinovsky E and Slunyaev A 2009 *Rogue Waves in the Ocean* (Springer, New York)
[14] Nott J 2006 *Extreme Events: A Physical Reconstruction and Risk Assessment* (Cambridge University Press, Cambridge)
[15] Onorato M *et al.* 2013 *Physics Reports* **528** 47-89
[16] Synolakis C E and Bernard E N 2006 *Phil. Trans. R. Soc. A* **364** 2231-2265
[17] Johnson R S 1997 *A Modern Introduction to the Mathematical Theory of Water Waves* (Cambridge University Press, Cambridge)
[18] Johnson R S 2003 *J. Nonlinear Math. Phys.* **10** 72
[19] Johnson R S 2012 *J. Nonlinear Math. Phys.* **19** 1240012
[20] Fedele R *et al.* 2008 *Frontier in Modern Plasma Physics. In: AIP Conf. Proc.*, **1061** (eds. P. K. Shukla, B. Eliasson, and L. Stenflo), p. 273
[21] Fedele R *et al.* 2009 *New Developments in Nonlinear Plasma Physics. In: AIP Conf. Proc.*, **1188** (eds. P. K. Shukla, B. Eliasson, and L. Stenflo), p. 365
[22] Hirota R 1979 *Phys. Lett. A* **71** 393
[23] Khusnutdinova K R, Klein C, Matveev V B and Smirnov A O 2013 *Chaos* **23** 013126, and references therein